

UDC 533.95, 507.9.

**HIGH CURRENT PLASMA ACCELERATORS: PHYSICS AND APPLICATIONS****I.E. Garkusha**\* *Institute of Plasma Physics of the National Science Center "Kharkov Institute of Physics and Technology  
Academicheskaya Street 1, Kharkov, 61108, Ukraine**E-mail: [garkusha@ipp.kharkov.ua](mailto:garkusha@ipp.kharkov.ua)*

Received 20 November 2012, accepted 24 January 2013

In this review paper, basic principles of high current plasma accelerators, history and recent state of their investigations in IPP NSC KIPT are briefly described. In such devices an internal magnetic field is created by high current up to several MA in the discharge and it is used for both plasma flow acceleration up to 1000 km/s. Particular attention is paid to the quasi-stationary plasma accelerators (QSPA), where discharge duration exceeds considerable the plasma flight time in acceleration channel. Application of QSPA for plasma-surface interaction studies relevant to thermonuclear reactors, like ITER and DEMO, is discussed. Results on surface modification and improvement of material properties by powerful pulsed plasma processing are described. Potential technological applications for materials treatment are emphasized.

**KEY WORDS:** plasma accelerator, high-energy streams of dense plasma, plasma-surface interaction, surface modification, extreme conditions of thermonuclear reactor ITER

**СИЛЬНОТОЧНЫЕ УСКОРИТЕЛИ ПЛАЗМЫ: ФИЗИКА И ПРИМЕНЕНИЕ****И.Е. Гаркуша***Институт физики плазмы, Национальный научный Центр «Харьковский физико-технический институт»  
Академическая, 1 61108, Харьков, Украина*

В данной обзорной работе кратко описаны основные принципы сильноточных ускорителей плазмы, история и современное состояние их исследований в ИФП ННЦ ХФТИ. В таких устройствах собственное магнитное поле создается большим током до нескольких МА в разряде и оно используется для ускорения потока плазмы до скоростей порядка 1000 км/с. Особое внимание уделено квазистационарным плазменным ускорителям (КСПУ), в которых продолжительность разряда значительно превышает время полета плазмы в ускорительном канале. Описаны эксперименты по применению КСПУ для исследований взаимодействия плазмы с поверхностью в термоядерных реакторах, таких как ИТЭР и ДЕМО. Представлены результаты исследований по модификации поверхности и улучшению свойств материалов при обработке мощными импульсными потоками плазмы. Подчеркиваются потенциальные технологические приложения импульсной плазменной обработки.

**КЛЮЧЕВЫЕ СЛОВА:** плазменный ускоритель, высокоэнергетичные потоки плотной плазмы, взаимодействие плазмы с материалами, модификация поверхности, экстремальные условия термоядерного реактора ИТЭР

**СИЛЬНОСТРУМОВІ ПРИСКОРЮВАЧІ ПЛАЗМИ: ФІЗИКА І ВИКОРИСТАННЯ****І.Є. Гаркуша***Інститут фізики плазми Національного Наукового Центру «Харківський фізико-технічний інститут»  
Академічна, 1 61108, Харків, Україна*

В даній оглядовій роботі коротко описані основні принципи сильнострумових прискорювачів плазми, історія та сучасний стан їх досліджень в ІФП ННЦ ХФТИ. У таких пристроях внутрішнє магнітне поле створюється великим струмом до декількох МА в розряді і воно використовується для прискорення потоку плазми до швидкостей порядку 1000 км/с. Особливу увагу приділено квазистационарним плазмовим прискорювачам (КСПП), у яких тривалість розряду значно перевищує час польоту плазми в прискорювальному каналі. Описано експерименти по застосуванню КСПП для досліджень взаємодії плазми з поверхнею в термоядерних реакторах, таких як ІТЕР і ДЕМО. Представлені результати досліджень по модифікації поверхні і поліпшення властивостей матеріалів при обробці потужними імпульсними потоками плазми. Підкреслюються потенційні технологічні застосування імпульсної плазмової обробки.

**КЛЮЧОВІ СЛОВА:** плазмовий прискорювач, високоенергетичні потоки щільної плазми, взаємодія плазми з матеріалами, модифікація поверхні, екстремальні умови термоядерного реактора ІТЕР

Plasma accelerators generating powerful dense plasma streams are able to be used for plasma injection into magnetic traps, investigations of plasma-surface interactions that can be occurred on the first wall or divertor plates during current disruption conditions and giant ELMs, for some technological applications related with modification and alloying of surface layers by plasma processing etc. In such devices an internal magnetic field is created by high current up to several MA in the discharge and it is used for both plasma flow acceleration up to 1000 km/s and also for dense magnetized plasma compression up to  $10^{19}$ - $10^{20}$  cm<sup>-3</sup>. The plasma acceleration (compression) can be organized in pulsed or quasi-stationary regimes. In first case the pulse duration typically is comparable with the time-of-flight of plasma ions in the accelerating channel. The acceleration process can be described in the frame of electrodynamic approximation either within "snow plough" model or "current sheath", for instance. The detailed information can be found elsewhere [1,2], therefore the electrodynamic approach will not be discussed here. Due to the high efficiency of plasma bunches acceleration combined with relative simplicity and robust design the pulsed plasma accelerators (PPA) are especially attractive for different technological applications related with materials processing etc. In quasi-

stationary plasma accelerators (QSPA) the discharge duration exceeds considerable the plasma flight time  $t_f$ . Supersonic plasma flow is kept during hundreds and thousands  $t_f$  and, practically, its duration of plasma stream generation is limited only by parameters of the power supply system used (capacitor battery) [3].

The main aim of this review paper is to describe briefly the basic principles of high current plasma accelerators and recent state of their investigations in IPP NSC KIPT. Application of QSPA for plasma-surface interaction studies relevant to thermonuclear reactors, like ITER and DEMO, is underlined. Results on surface modification and improvement of material properties by powerful pulsed plasma processing are emphasized aiming at potential technological applications for materials treatment.

### GENERAL PRINCIPLES OF QUASI-STATIONARY PLASMA FLOWS IN ACCELERATING CHANNELS

The general principles of quasi-stationary acceleration of high-power plasma streams have been formulated by Morozov [3,4] on the base magneto-hydrodynamics (MHD) approach, proposed by H. Alfven. In the frame of one-fluid MHD model the plasma flow acceleration due to the thermal and magnetic forces can be described by following system of equations:

$$\rho \left( \frac{\partial \vec{v}}{\partial t} + (\vec{v} \nabla) \vec{v} \right) = -\nabla p + \frac{1}{c} [\vec{j}, \vec{H}] \quad (1)$$

$$\frac{\partial \rho}{\partial t} + \text{div} \rho \vec{v} = 0 \quad (2)$$

$$\vec{j} = \frac{c}{4\pi} \text{rot} \vec{H} \quad (3)$$

$$\text{div} \vec{H} = 0 \quad (4)$$

$$\frac{\partial \vec{H}}{\partial t} = \text{rot} [\vec{v}, \vec{H}] \quad (5)$$

$$p = p_0 \left( \frac{\rho}{\rho_0} \right)^\gamma \quad (6)$$

Here  $\rho$ ,  $p$ , and  $v$  are density, pressure and velocity in plasma stream, index zero corresponds to entrance of the accelerating channel;  $J, H$  are electric current density and magnetic field.

In the case of stationary axial-symmetric flow:  $\frac{\partial}{\partial t} = 0$ ,  $H_r = H_z = 0$ ,  $v_\theta = 0$ .

The plasma flow is divided into narrow flux tubes with a width  $h = h(z)$ . Under these assumptions three conservation laws (holding true for each flux tube) follow from the above system of equations:

$$\frac{v^2}{2} + \int \frac{dp}{\rho} + \frac{H^2}{4\pi\rho} = \text{const} \equiv U \quad (7)$$

Where,  $i(\rho) \equiv \int \frac{dp}{\rho} = \frac{p_0}{\rho_0} \frac{\gamma}{\gamma-1} \left( \frac{\rho}{\rho_0} \right)^{\gamma-1}$  is enthalpy,

$$\frac{H}{\rho} = \text{const} \equiv k \quad (8)$$

$$\rho v h = \text{const} \equiv \dot{m} \quad (9)$$

First one is well known Bernoulli equation that expresses the conservation of full energy in the flow. Second conservation law describes freezing-in azimuth magnetic flux into a plasma. And last one is mass conservation in the tube, resulting from continuity equation (2).

From (9) it follows that the acceleration channel width  $h = \frac{\dot{m}}{\rho v}$  for any chosen mass flow rate  $\dot{m}$  tends to

infinity at both input and output of the channel, where  $\rho \rightarrow 0, v \rightarrow v_{\max}$  and  $\rho \rightarrow \rho_0, v \rightarrow 0$  correspondingly. Therefore it should have a minimum in some so called "critical section", in analogy with profiled Laval nozzle.

In such MHD analog of Laval nozzle transition through the sound velocity occurs in critical section, and the sound's velocity role plays Alfven velocity  $C_A = H / (4\pi\rho)^{1/2}$ . Maximal plasma stream velocity at the output of acceleration channel is  $v_{\max} = (2)^{1/2} C_{A0} = H_0 / (2\pi\rho)^{1/2}$ , being fully defined by input parameters and giving potential possibility to achieve plasma streams with very large ion energies.

However, experimental realization of quasi-stationary plasma flows in discharges with solid (non-transparent)

electrodes showed severe restrictions related with the effect of “the discharge current crisis”, strong erosion of electrodes, both anode due to the electric potential jump and cathode, due to the bombardment by ions [4]. Also instability of ionization zone led to the overloading the electrodes in insulator in the high current discharge.

An important step to solve these problems is related with the proposed physical concept of quasi-stationary plasma accelerator (QSPA) based on ion carried electric current in the acceleration channel and electrodes-transformers [4-7]. Briefly, QSPA concept proposed by A.I. Morozov in Kurchatov Institute, Moscow and experimentally realized in IPP NSC KIPT, Kharkov involves: 1) the transition to a two-stage scheme of acceleration in order to eliminate the influence of instability of the neutral gas ionization region; 2) the transition to the mode of operation, under which the electric discharge current in the main accelerating channel is carried by ions, thus providing for the best match of equipotential electrodes with electric and magnetic fields in the plasma stream; 3) magnetic screening of solid-state electrode components. The transition to the condition of discharge current transport by the ions significantly complicates the functions of electrodes, where the replacement of current carriers, namely, electrons in the accelerator's power supply circuit by ions in the plasma, should take place. Besides, the ions must be supplied to the accelerating channel on the anode side and be removed on the cathode side. So, the electrodes of a quasi-stationary high-current plasma accelerator would be magneto-plasma electrodes - transformers of a complicated design, which provide both the magnetic screening of their solid-state components and the conditions for accomplishing the regime of current transport by ions.

### EXPERIMENTAL STANDS OF HIGH CURRENT PLASMA ACCELERATORS

Above described concept has been verified in QSPA of a simplified design with rod-like electrodes [4-7] and later on in full-block QSPA [8-10]. Those experiments have demonstrated the feasibility of the quasi-stationary mode of acceleration with quasi-radial current lines, that was lasting for about 20 to 30  $\mu\text{s}$  (at a discharge length of  $\sim 300 \mu\text{s}$  for QSPA with passive transformers (QSPA P-50) and more than 200  $\mu\text{s}$  for QSPA Kh-50. One can see such systems are prospective from the point of view of plasma generation with super high energy contentment in steady (quasi)-stationary operational regime. Up to now, when using full-block QSPA Kh-50, plasma streams with the mean proton energy  $\leq 0.9 \text{ keV}$ , plasma energy density up to  $2 \text{ kJ/cm}^2$ , mean plasma density  $(3-5) \times 10^{16} \text{ cm}^{-3}$ , plasma stream diameter up to 50 cm, total energy of plasma stream  $\leq 600 \text{ kJ}$ , the time duration of quasi-stationary phase of acceleration  $\geq 200 \mu\text{s}$  with total pulse length  $\approx 300 \mu\text{s}$  are generated.

Plasma characteristics of three types of accelerators being in operation in IPP are shown in Table 1. The characteristics of the plasma flow in the accelerating channel as well as the parameters of the generated plasma streams were in strong dependence on the conditions on the electrodes.

Table 1.

Characteristics of the experimental devices

Installations	QSPA Kh-50	QSPA P-50	PPA
	Full-Block Quasi-Stationary Plasma Accelerator	Quasi-Stationary Plasma Accelerator with Passive Electrodes	Pulsed Plasma Accelerator
Parameters			
Mean ion energy, keV	$\leq 0.9$	$\leq 0.2$	$\leq 5.0$
Plasma stream density, $\text{cm}^{-3}$	$\leq 5.10^{16}$ (Z=0.5 m) $\leq 2.10^{15}$ (Z=3.0 m)	$\leq 2.10^{16}$ (Z=0.5 m) $\leq 10^{15}$ (Z=2.0 m)	$\leq 10^{15}$ (Z=0.5 m)
Electron temperature, eV	$\leq 4$	$\leq 4$	$\leq 50$
Plasma stream energy, kJ	$\leq 600$	$\leq 40$	$\leq 10$
Plasma energy density, $\text{J/cm}^2$	2000 (Z=0.5 m) 200 (Z=3.0 m)	$\leq 120$ (Z=2.0 m)	$\leq 40$
Mean plasma diameter, cm	$\leq 20$ (Z=0.5 m) $\leq 100$ (Z=3.0 m)	$\leq 10$ (Z=0.5 m) $\leq 40$ (Z=2.0 m)	$\leq 15$
Plasma discharge duration, $\mu\text{s}$	300	300	5
Plasma stream generation duration, $\Delta\tau_p$ , $\mu\text{s}$	$\leq 150$	$\leq 40$	$\leq 3$
Main discharge capacitor bank Capacity, C, $\mu\text{F}$	7200	5600	111
Voltage, U, kV	$\leq 15$	$\leq 8$	$\leq 30$

Schematic and general view of experimental stand of QSPA Kh-50, that is largest and most powerful device of this kind, is presented in Fig. 1. Electrodes configuration of QSPA P-50 and typical image of generated plasma stream are shown in Fig. 2. General view of upgraded PPA stand of pulsed plasma accelerator adjusted for technological tasks is shown in Fig. 3.

The full-block powerful quasi-steady-state plasma accelerator QSPA Kh-50 consists of two stages. The first one is used for plasma production and pre-acceleration. The second stage (main accelerating channel) is a coaxial system of shaped active electrodes-transformers with magnetically screened elements (those elements are current supplied either

from independent power sources or branching partly the discharge current in self-consistent regime of operation). The maximum total energy of capacitor banks supplying all active elements of the QSPA achieved 4 MJ. Design of accelerator is described in details in [8-11]. Plasma streams, generated by QSPA Kh-50 are injected into magnetic system of 1.6 m in length and 0.44 m in inner diameter consisting of 4 separate magnetic coils. The first magnetic coil is placed at the distance of  $Z_S = 1.2$  m from accelerator output. The currents in each coil are specially selected to provide plasma streams propagation in slowly increasing magnetic field. The maximum value of magnetic field  $B_0=0.7$  T was achieved in diagnostic chamber  $Z_S = 2.2-2.4$  m from accelerator output.

The instrumentation for diagnostics of plasma flow in the accelerating channel and the parameters of the generated plasma streams includes a set of Rogowski coils, frequency-compensated voltage dividers, electric and magnetic probes, piezodetectors, bolometer, local movable calorimeters, high-speed cameras in different modifications, time-of-fly energy analyzer. The plasma stream density was determined from the Stark broadening of the  $H_\beta$  and self-absorption  $H_\alpha$  spectral lines, or spectral lines of He, Ar, N [12], and also by using the autocollimation interferometer with view area of 200 mm in diameter. The velocity of different parts of the plasma stream was measured on the basis of time-dependent modulation of radiation using the slit scanning and registration by a high-speed camera, as well as by measuring the Doppler shift of spectral lines CII ( $\lambda=4267$  Å) and self-absorption  $H_\alpha$  (when working with hydrogen), or HeII ( $\lambda=4686$  Å) and CII ( $\lambda=4267$  Å) (for helium), or ArII ( $\lambda=6643$  Å) and NII ( $\lambda=4630$  Å) (when working with argon and nitrogen, respectively). Electron temperature was evaluated by the ratio of spectral lines intensities, or by the analysis of contours of self-absorption spectral line  $H_\alpha$ .

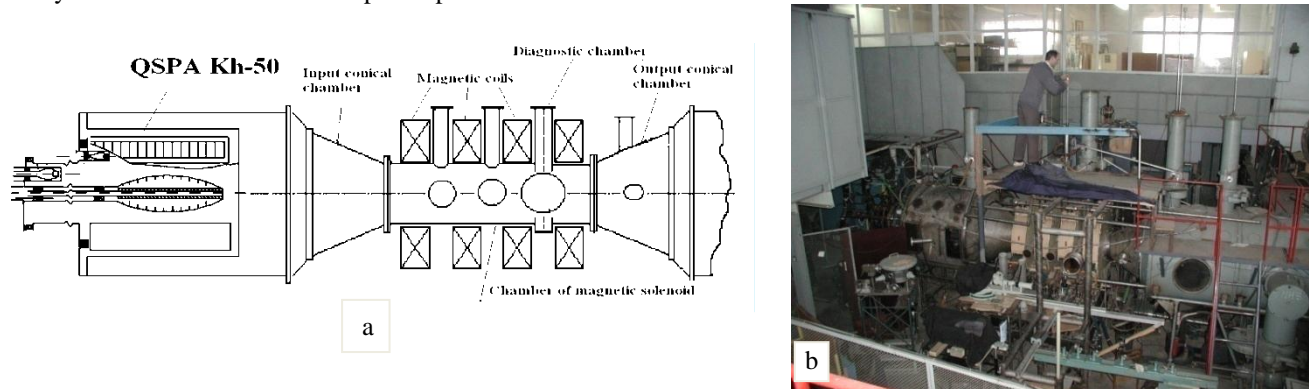


Fig.1. QSPA Kh-50 experimental stand

a – scheme, b - general view.

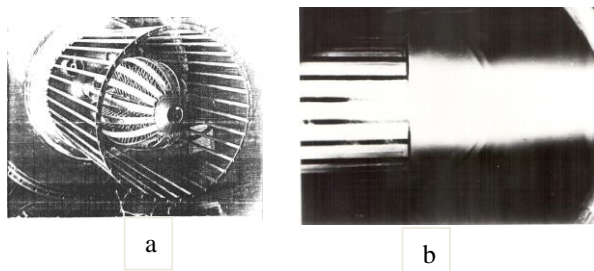


Fig.2. Electrodes of QSPA P-50 (a) and plasma stream photo (b).

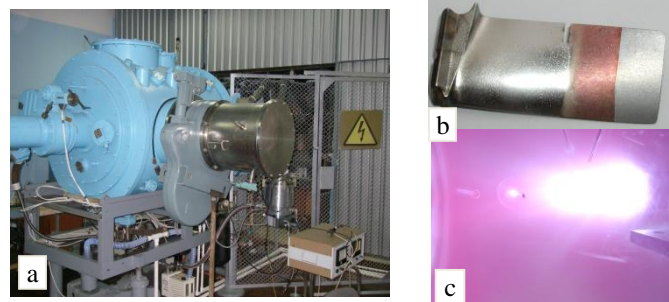


Fig.3. Upgraded PPA stand of pulsed plasma accelerator adjusted for technological tasks (a), plasma plume (c) and treated sample (b)

### QSPA APPLICATION FOR SIMULATION OF TRANSIENT EVENTS IN ITER TOKAMAK-REACTOR

Experimental investigations of plasma-surface interaction (PSI) in conditions simulating transient events in fusion reactor ITER are of importance for the determination of erosion mechanisms of plasma facing materials, dynamics of erosion products, the impurities transport in the plasma, the vapor shield effects and its influence on plasma energy transfer to the material surface. In turn, the obtained results are used for validation of predictive models developed for ITER and DEMO, estimation of tolerable size of Type I ELMs and lifetime of divertor armour materials.

Energy range of ITER disruptions is  $Q_{\text{disr}} = (10-100)$  MJ/m<sup>2</sup>,  $t = 1-10$  ms. This is two orders of magnitude higher being far above of that in available tokamaks. Therefore, at present for experimental study of plasma-target interaction under the high heat loads the powerful plasma accelerators and other powerful simulators are applied [13,14]. Quasi-stationary plasma accelerators (QSPA), which are characterized by essentially longer duration of plasma stream in comparison with pulsed plasma guns, are especially attractive for investigations of macroscopic erosion of tokamak armor materials under the loads expected at ITER off-normal events. In turn, the obtained experimental results are used for validation of the predictive numerical models. Therefore, largest in the word QSPA Kh-50, became unique and

practically most adequate simulator of plasma-surface interaction during ITER transient events, resulting in huge energy densities impacting to the divertor material surfaces.

Extrapolation of the ELMs erosion effects obtained at the present-day tokamaks to the transient peak loads of ITER remains uncertain. Experimental observations from different machines pointed out similarities and the open questions, which require further investigations are overviewed in [15,16]. The obtained power loads associated with the Type I ELMs generally do not affect the lifetime of divertor elements. However, the ITER ELMs may lead to unacceptable lifetime; their loads are estimated as  $Q_{ELM} = (1-3) \text{ MJ/m}^2$  at  $t = 0.1-1 \text{ ms}$  and the repetition frequency of an order of 1 Hz ( $\sim 400$  ELMs during each ITER pulse. Special investigations on material behavior at the ELM relevant loads (both numerical and experimental) are thus very important.

In disruption and ELMs simulation experiments with QSPA Kh-50, the plasma stream parameters were varied by both changing the dynamics and quantity of gas filled the accelerator channel and changing the working voltage of capacitor battery of the main discharge. To achieve the working regimes for simulation both the disruptive and ELM-like plasma impacts, the main attention in these experiments was paid to possibility of effective variation of plasma stream energy density in wide range and determination of target heat load in dependence on plasma stream energy density.

Plasma parameters measured for 2 working regimes with plasma energy density of about  $1 \text{ MJ/m}^2$  and  $25-30 \text{ MJ/m}^2$  respectively, which were chosen for simulation experiments, are summarized in Table 2. Taking into account essentially longer duration of the thermal quench of ITER disruption, for disruption simulation regime special efforts were done to increase the plasma pressure in QSPA plasma stream up to 1.6-1.8 MPa. As it was shown in [17], this allowed to make clear the influence of plasma pressure gradient on melt motion even for QSPA plasma pulse duration and to approach the melt velocities to those expected for ITER disruptions.

Table 2.

Main parameters of QSPA Kh-50 plasma streams in different working regimes

	Disruption simulation regime	ELM simulation regime
Discharge duration [ms]	$\sim 0.3$	0.28
Power pulse half-height width [ms]	0.1-0.14	0.1-0.12
Heat input [ $\text{MJ/m}^2$ ]	25-30	0.9-1.5
Heat load on sample surface [ $\text{MJ/m}^2$ ]	0.65-1.1	0.45-0.75
Maximal plasma stream pressure [MPa]	1.6-1.8	0.48
Average plasma density [ $10^{16} \text{ cm}^{-3}$ ]	4-8	1.5-2.5
Ions energy [keV]	$\sim 0.6$	$\sim 0.2$
Spot size of treated surface [cm]	10-12	12-14

### Vapor shield effects

The key feature of plasma-surface interaction under disruption heat loads is vapor shield formation in front of material surface. Temporal and spatial distributions of plasma density in the shielding layer have been obtained with laser interferometry. Fig. 4. shows typical interferometric picture of high power plasma stream interaction with graphite surface and shielding layer in the vicinity of target surface. The plasma density in the shield is more than one order of magnitude higher in comparison with that in impacting plasma stream. Spatial distribution of electron density strongly depends on the energy density of the plasma stream and target size. The thickness of the shielding layer, formed close to the graphite target under normal irradiation of surface with plasma energy density of  $25 \text{ MJ/m}^2$ , which is expected for ITER disruptions, can be evaluated from Fig. 4. The figure shows that shielding layer thickness, being equal (1-2) cm for sample irradiation with no magnetic field, is exceeded 5 cm for  $B_{z0} = 0.72 \text{ T}$ . The thickness of shielding layer grows with increasing magnetic field value and time of plasma interaction with a target.

Formation of dense plasma layer in front of the surface protects the material from the contact with impacting plasma. Thickness of the shielding layer essentially exceeds the particles free path. Shielding efficiency of carbon vapor is analyzed in [10,14], and, typically, only few percents of impacting plasma energy reaches the surface for disruption plasma loads. Dissipation of the plasma stream energy in the shielding layer results in shield expansion, heating and re-irradiated by the shield. Intense radiation from the shield may affect to the nearby surfaces of the ITER divertor, which are not contacted with plasma.

Measurements of radiation from the plasma shield in wavelength range of  $\lambda \leq 3000 \text{ \AA}$  have been performed with pyroelectric bolometer in regime of radiative calorimeter (Fig. 5). It is shown intensity of radiation from the shielding layer is in 7-10 times higher in comparison with free plasma stream (Fig. 6). Maximum of radiation is registered not from the near surface layer, but from thin region of  $\sim 5 \text{ mm}$  corresponding to periphery zone of the shielding layer (2-3 cm from the surface) being contacting with impacting plasma stream.

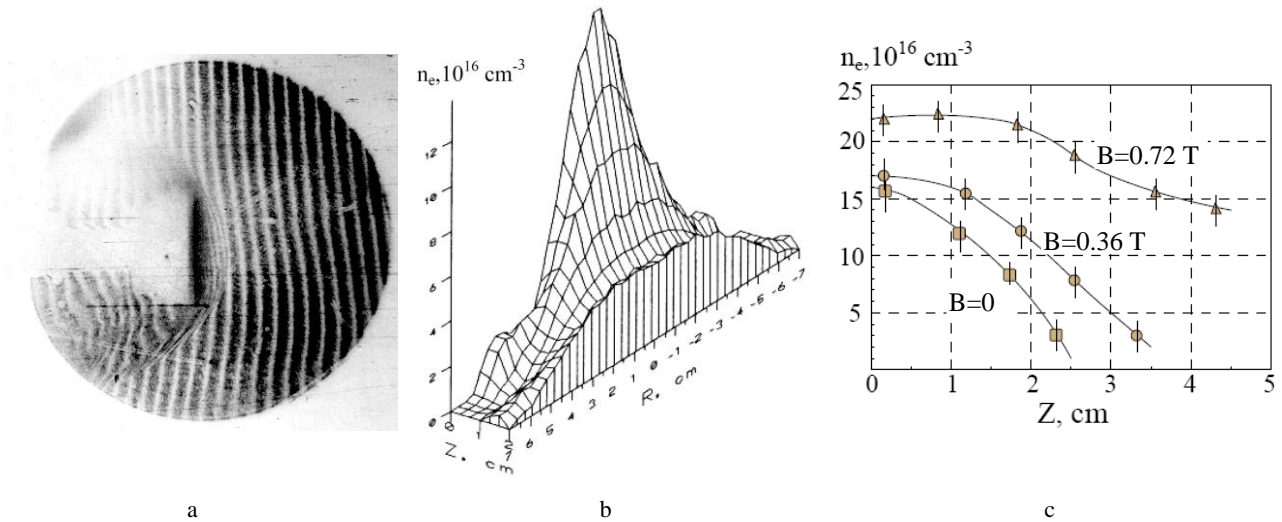


Fig. 4. Formation of vapor shield in front of the exposed surface  
 a - interferometric picture of plasma stream interaction with graphite target; b,c- electron density distributions in plasma shield.  
 $E=25 \text{ MJ/m}^2$ ,  $\Delta\tau=20 \text{ }\mu\text{s}$  from the beginning of plasma interaction with the surface.  $Z=0$  corresponds to the target surface

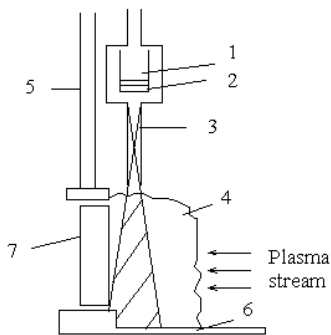


Fig. 5. Scheme of the bolometric measurements. 1 -  $\text{LiNbO}_3$  detector, 2 -  $\text{LiF}$  filter, 3 - diaphragms, 4 - shielding layer, 5 - holder, 6 - restrictor, 7 - target

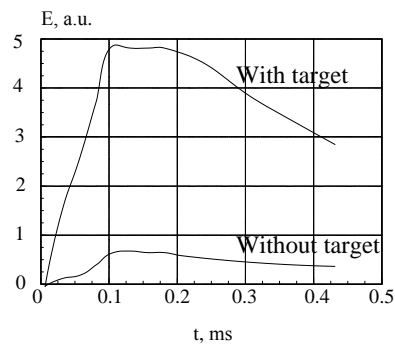


Fig. 6. Intensity of radiation from the plasma stream and shielding layer in front of the target.

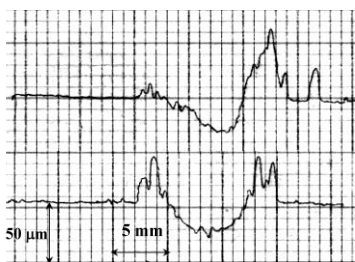


Fig. 7. Melt layer profiles on the exposed inclined surface in direction of inclination (upper) and in perpendicular direction (lower). Inclination angle  $\alpha=20^\circ$ .

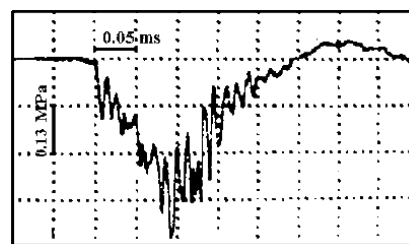


Fig. 8. Temporal behavior of plasma pressure in ELM simulation experiments.  $Z=2.3 \text{ m}$  from accelerator output.

In spite of strong shielding, any metal surface will be subjected to strong melting during the disruption. The melt layer is subjected to external forces such as surface tension, gradients of both plasma pressure and recoil pressure of evaporating material, Lorentz force and others. The disruption simulation experiments with QSPA Kh-50 have shown that melt motion driven by external forces produces significant macroscopic erosion of materials. In particular, melt layer motion driven by plasma pressure results in erosion crater formation with rather large mountains of the resolidified material at the crater edge. Example of erosion crater appeared due to the melt motion on the metal surface exposed with inclined plasma stream impact is presented in Fig. 7.

### Impacts of repetitive ELMs

Plasma pressure during ITER ELMs is anticipated to be essentially lower in comparison with disruptions. Therefore one possible to expected much smaller effects from the melt motion. In this case other macroscopic mechanisms such as brittle destruction and cracking may dominate the erosion, exceeding essentially contribution from microscopic mechanisms like sputtering or even evaporation.

ELM-simulation regimes in QSPA Kh-50 are characterized by experimentally chosen heat loads, which do not lead to the surface melting for tested tungsten samples, or result in melting initiation. Describing the plasma stream parameters for this regime it should be mentioned in addition to the data of Table 2, that triangular shape of plasma heat load has been realized. This simple shape is quite suitable for simulation of ITER ELM impacts. Temporal dependence of plasma pressure for this regime is presented in Fig. 8. Duration of plasma stream achieved 0.25 ms.

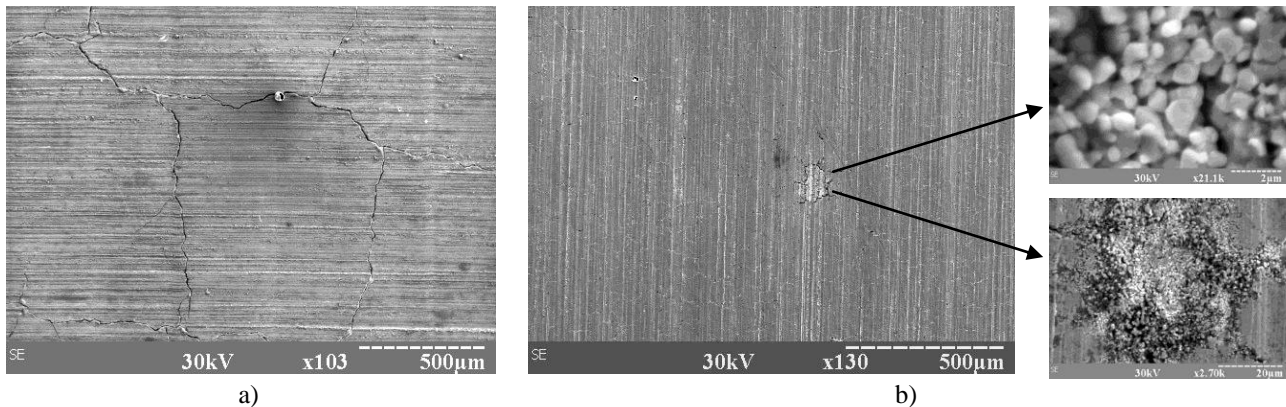


Fig. 9. Tungsten surface after 210 plasma pulses of  $0.45 \text{ MJ/m}^2$ .  
a) - RT target, b) - preheated target 650 C with enlarged images of the surface damage.

Examples of tungsten material damage below the melting threshold in ELM simulation experiments are presented in Fig. 9 for samples with different initial temperatures. Tungsten is primary choice for ITER divertor armour and even candidate for the DEMO first wall and divertor. It has highest melting temperature, low sputtering yield large sputtering threshold energy. Tritium retention in tungsten is also acceptable. However, main drawback is that tungsten is brittle material under moderate temperatures, the ductile-to-brittle transition temperature (DBTT) for some W grades may achieve 200-600 C. Brittleness of W gives rise to surface cracking. To minimize the brittle destruction erosion, the W-armor have to be kept above the DBTT. Analysis of effects of W temperature on material damage under ELMs impacts requires comprehensive experimental studies that now in progress in many fusion laboratories [18,19].

It is seen from Fig. 9, that for room temperature target the mesh of major cracks is developed on the surface, while for the material preheated to 650 C, the macro-cracks are absent. Nevertheless micro-cracks are registered on preheated surface. Thus, it is shown that tungsten cracking can not be completely mitigated by the preheating above the DBTT, but it can be essentially minimized, especially under the irradiation below the melting threshold. Tungsten preheating above DBTT allows suppressing the macrocracks formation on the surface. After first hundred of plasma pulses only microcracks were found and it can be classified as fatigue cracks resulting from repetitive stresses induced by numerous plasma impacts. Large number of pulses results also in surface modification (Fig 9,b) and formation of submicron structures. With further pulses such structures occupy all the surface and the tungsten, melting point decreases due to decreased heat conductivity in the modified layer. The surface became significantly damaged even after exposures with quite small energy loads.

Evolution of preheated tungsten surface as a result of plasma loads causing surface melting is demonstrated in Fig. 10. As follows from microscopy observation the surface is rather stable with increasing number of exposures up to 100-130 pulses. A blister-like structures and bubbles with the size of 100-300 μm are arisen on the surface after 100 pulses. The balls of nano size are registered inside the blister voids and in the crack volumes. Their size is varied within 10 nm - 1 μm. Surface modification with formation of cellular submicron structures is also occurs.

The most important changes in surface morphology are observed after increase of the exposition dose above 200 pulses, which results in qualitative evolution of the surface similar to that observed for exposures of RT targets in regimes with the same heat load of  $0.75 \text{ MJ/m}^2$  and with the heat load of  $1.1 \text{ MJ/m}^2$  (corresponds to the evaporation start) after similar number of pulses. The obtained results show that after the threshold number of exposures qualitative evolution of the surface is practically the same for all the cases mentioned above.

Due to the corrugations, the initially uniform melt layer tends to be transformed into “shagreen leather”. The width of the micro-cracks gradually increases with increasing the number of exposures, achieving 0.8-1.5 μm after 100 pulses and up to 20 μm after 200 pulses. Initially, the fine network of the cracks is remelted from pulse to pulse. With increasing width of the intergranular cracks, the surface became micro-brush-like, where surface areas of 20-50 μm are separated from each other. The following remelting with next pulses does not result furthermore in mixing because of the increased depth and width of the cracks and negligible melt motion during single pulse. Being separated, each cell

of the cracks network subjected to action of the surface tension directed to the minimization of cell area and under the large number of repetitive exposures the total contribution of plasma pulses results in progressive corrugation of the surface.

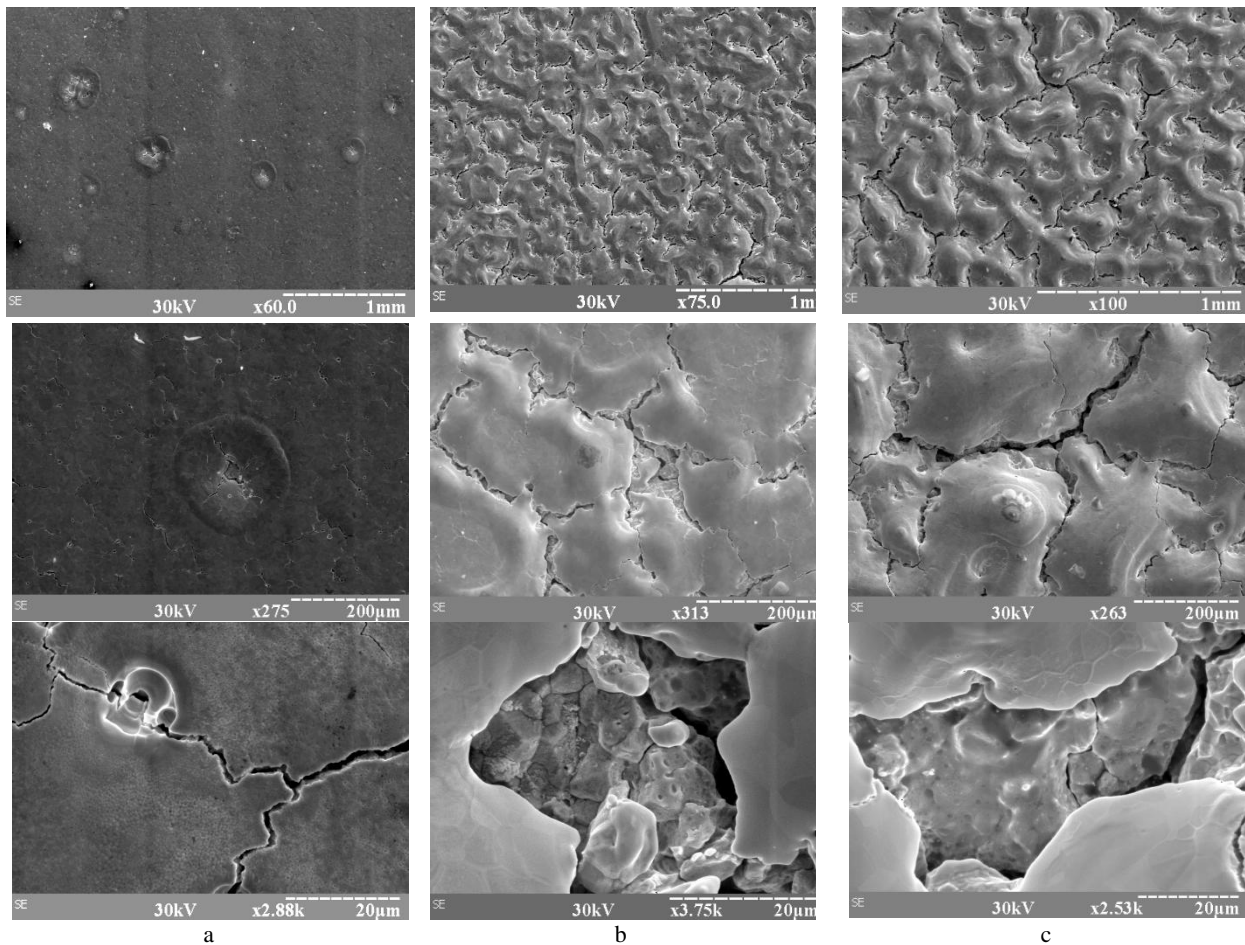


Fig. 10. SEM images of the tungsten surface  
a – after 100, b – after 210, and c - after 350 pulses with different magnification

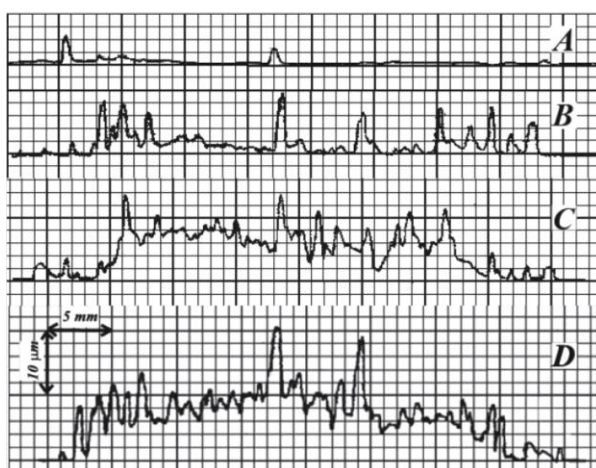


Fig. 11. Evolution of surface profiles of preheated tungsten in the course of plasma exposures.  
A - 80 pulses, B - 150 pulses, C - 210 pulses, D - 350 pulses

plasma parameters in front of the exposed surfaces for normal and inclined plasma stream incidence, impurities dynamics in near-surface plasma and energy deposited to the material surface. Particular attention is paid to the material erosion due to particles ejection from the tungsten surfaces both in the form of droplets and solid dust.

The erosion products flying from the tungsten target have been registered using high-speed 10 bit CMOS digital

Further evolution of the surface pattern is caused by loss of separated grains on exposed surface with increased number of impacts. It is seen that in result of 350 pulses (Fig.10,c) the surface became essentially destroyed by cracks. Thus, the damage, caused by cracking, became dominating after several hundreds of exposures, even for preheated target. The microscopy observations well correlate with profile measurements. The profile swelling, which is registered after 200 pulses, is caused by threshold changes in surface morphology (Fig.11).

#### Mechanisms of dust generation

Another important issue in ELM simulation experiments is generation of W dust in result of plasma impacts. The dust particles may penetrate in to the plasma core and thus to cool immediately the plasma. Also tritium retention due to developed surface area in dust layers has to be clarified. Performed studies of plasma-surface interaction in QSPA Kh-50 included measurements of

camera pco.1200 s from PCO AG with the exposure time  $1\ \mu\text{s} \dots 2\text{ms}$ , spectral range  $290 \dots 1100\ \text{nm}$  and space resolution of  $1280 \times 1024$  pixels. Information from several camera frames with traces of particles flying from the tungsten surface after plasma shot (Fig. 12) allow calculation of the particles velocity and the time moment when it started from the target surface. Additionally the mass loss of the target was measured after several shots. Erosion products ejected in the form of droplets and solid dust were also collected and examined with microscopy.

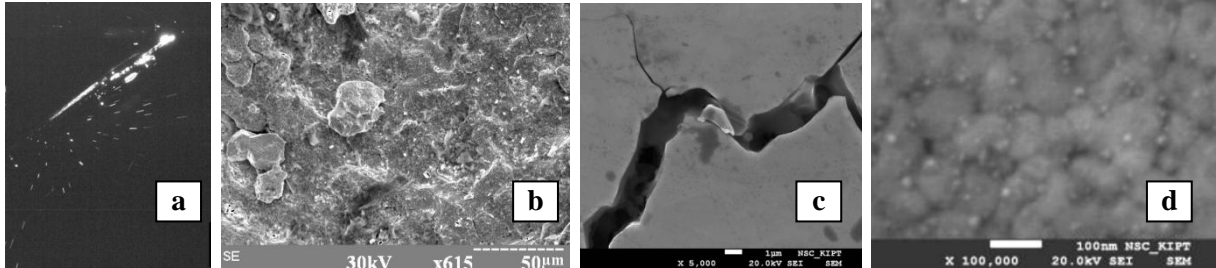


Fig. 12. Dust particles traces from inclined W target (a) and collected dust resulted from grain losses (b), cracking development (c) and W nano-powder due to the surface modification (d).

In recent studies with QSPA Kh-50 several mechanisms of dust generation under the transient energy loads to the tungsten surfaces have been recognized and identified basing on dust dynamics analysis, and particles characterization. Dust particles with sizes up to tens  $\mu\text{m}$  are ejected from the surface due to the cracking development and major cracks bifurcation. This mechanism would be dominating for first transient impacts when major crack mesh is formed. The energy loads in this case may not result in the melting, but it have to be above the cracking threshold. Taking into account that for many repetitive pulses the cracking threshold shifts to smaller energy loads, this mechanism can only be enfeebled by tungsten preheating above the ductile-to-brittle transition temperature. Fatigue cracks are still able to be developed after a large number of transient impacts to the preheated W surface [19]. This is a source of smaller dust. For plasma exposures with energy loads above the melting threshold both droplets splashing and solid dust ejection is observed. Melting of surface and development of fine meshes of cracks along the grain boundaries are accompanied by resolidified bridges formation through the fine cracks in the course of melt motion and capillary effects. With next impacts (even without melting) such bridges produce nm-size W dust. For this mechanism the mass taken away by any single particle is much smaller, but the number of dust particles is considerable.

Furthermore, even if mitigated cracking, the effects of surface modification of tungsten material after the repetitive plasma pulses with development of ordered submicron cellular structures [21] are able to contribute significantly to the nm-dust generation (Fig. 13). However the obtained experimental results show that majority of generated dust nano-particles, generated due to cells evolutions, are deposited back to the surface by a plasma pressure, in contrast to  $\mu\text{m}$ -size dust. This result is confirmed by spectroscopy measurements of W impurities in plasma in front of the surface. The results of QSPA plasma exposures are compared with short pulse PSI experiments ( $\tau \sim 0.1\text{-}5\ \mu\text{s}$ ) with pulsed plasma gun and dense plasma focus facilities [22], aiming at features of surface damage and tungsten impurities behaviour in near-surface plasma in front of the target.

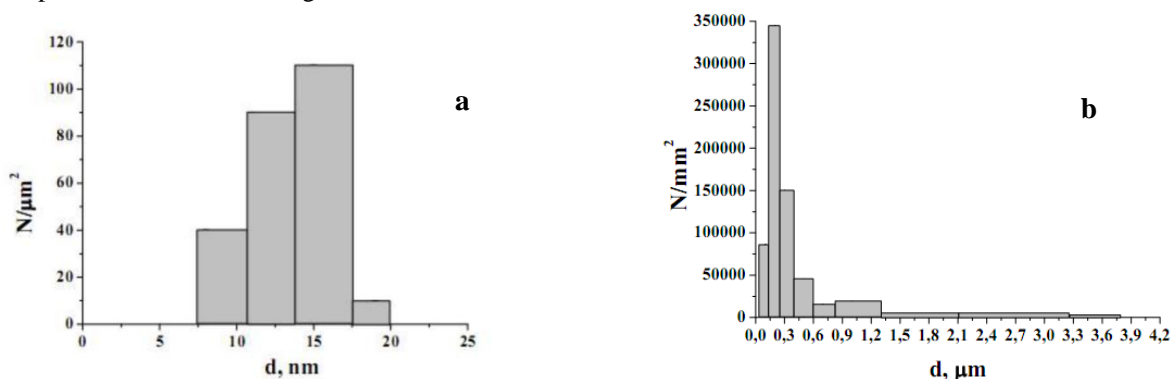


Fig. 13. Size distributions of W nano-particles (a) and collected W balls in crack voids (b)

#### MATERIALS MODIFICATION WITH POWERFUL PULSED PLASMA PROCESSING: FROM SURFACE DAMAGE TO THE MATERIAL IMPROVEMENT

Surface processing with pulsed plasma streams of different gases under moderate energy density range is found to be effective tool for modification of surface layers of various steel materials [23-26]. In particular, exposures with pulsed powerful plasma streams result in hardening their surfaces and increasing the wear resistance of industrial steels. In such “intelligent” regimes of plasma treatment the energy densities are adjusted to produce surface modification rather than erosion. Typically the heat load to the surface is above the melting threshold but essentially lower the

evaporation limit. Fast heating and melting of treated surface, considerable temperature gradients ( $\sim 10^6$  K/cm) arising in surface layer of material under the pulsed plasma impact contribute to high speed diffusion of plasma stream ions into the depth of the modified layer, during the liquid stage, phase changes in the surface layer, and formation of the fine-grained or quasi-amorphous structures under the following fast resolidification. The cooling speed of  $\sim 10^6$ - $10^7$  K/s is achieved in this case due to the contact of thin melt layer ( $h_{\text{melt}} \sim 10$ - $50 \mu\text{m}$ ) with massive bulk of the sample. Plasma can also be considered as a source of alloying elements to be introduced into modified layer structure. That is why nitrogen is preferentially used for pulsed plasma processing of different steels. Another possibility of alloying under the pulsed plasma processing is mixing of previously deposited thin ( $h_{\text{coat}} < h_{\text{melt}}$ ) coatings of different predetermined composition with the substrate in result of powerful plasma impact.

Examples of modified surface layer structures for different materials are presented in Fig. 14. Analysis of samples cross-sections was performed for different materials processed with helium, oxygen and nitrogen plasma streams. Adjustment of plasma treatment regimes of processed materials was done to achieve optimal thickness of modified layer with simultaneously minimal value of surface roughness. Depth of aluminium modified layer under oxygen plasma treatment achieved  $50 \mu\text{m}$ , microhardness in modified layer  $\sim 316 \text{ kg/mm}^2$ .

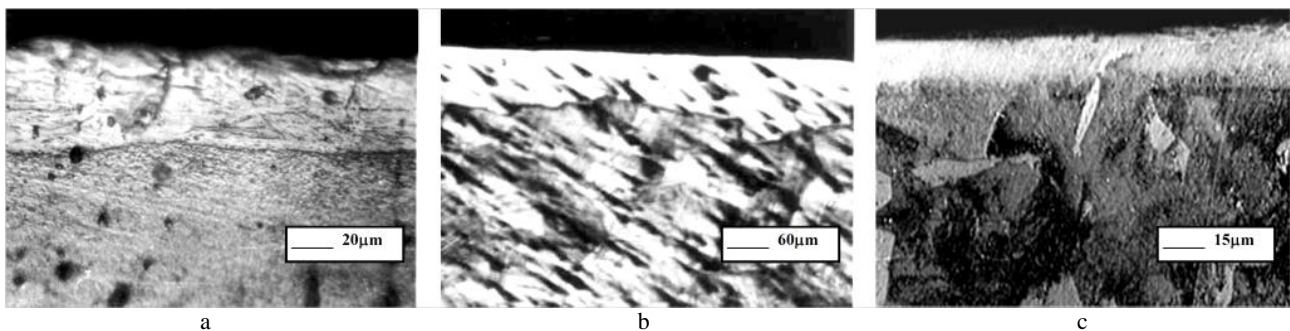


Fig. 14. Cross-sections of processed materials

a - Al processed with oxygen plasma, b - Ti-alloy VT22 processed with helium plasma, c - steel 40H processed with nitrogen plasma.

Using the light-weight gas for material treatment allowed to increase both pulse duration (up to  $10$ - $15 \mu\text{s}$ ) and energy density load to the sample surface (up to  $50 \text{ J/cm}^2$ ). Therefore it was possible to increase the depth of modified layer for titanium alloy samples up to  $100 \mu\text{m}$  under processing with He plasma streams. Modified layer of titanium alloy is not polarised and possibly consist on amorphous or  $\beta$ -Ti.

For different steels treatment with pulsed nitrogen plasma streams, it was formation of  $\gamma$ -Fe and nitrides as well as increase in the quantity of nitrides (mainly of  $\epsilon$ -Fe<sub>2</sub>N) with increasing dose of the treatment. Stabilization of  $\gamma$ -Fe in modified layer was determined mainly by high temperature heating the surface under plasma processing and rapid cooling. However the quantity of nitrides is strongly depended on concentration of chromium, nickel and other alloying elements. The decrease of  $\alpha$ -Fe lattice period and its increase for  $\gamma$ -Fe, decreasing the relative intensities of diffraction lines of phases  $\alpha$ -Fe and  $\gamma$ -Fe, broadening of diffraction profiles can be considered as typical feature of processing by pulsed plasma streams. This can be attribute of surface amorphization.

More detailed studies of modified steels with CEMS spectroscopy revealed that modification of surface layer accompanied only partially by  $\gamma$ -Fe, but it is attributed mainly by formation of  $\gamma_N$  phase [27]. This phase has been named as oversaturated austenite, i.e austenite in which an Fe atom has an interstitial nitrogen atom in the nearest neighbor.

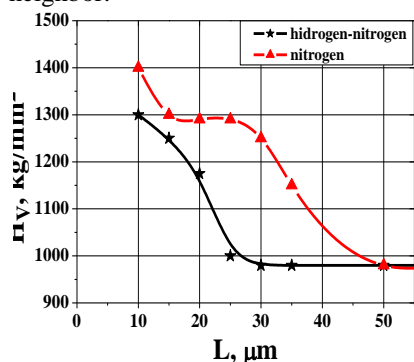


Fig. 15. Microhardness depth profiles of WC-20Co samples

changes of phase composition of the modified layer in result of repetitive heating and cooling under pulsed plasma heat loads [28].

Fig. 15 shows microhardness dependence on the depth of modified layer for the plasma treated WC-20Co samples. It should be noted that pulsed plasma processing with impacting particle dose of  $5 \cdot 10^{18} \text{ ion/cm}^2$  leads to increasing microhardness from  $1000 \text{ kg/mm}^2$  to  $1400 \text{ kg/mm}^2$ . Thickness of the layer with increased microhardness achieved  $50 \mu\text{m}$ . Maximum value of  $H_v \approx 1300 \text{ kg/mm}^2$  is observed WC-20Co surface in result of exposure with plasma stream which consists of the mixture of hydrogen and nitrogen in proportion of 1:1 and with the same dose of  $5 \cdot 10^{18} \text{ cm}^{-2}$ . Similar increase has been observed after pure hydrogen plasma exposures. This means that in this case microhardness changes are probably caused by high-speed plasma quenching, i.e. predominantly thermal effects and only minor influence of nitriding on the microhardness behaviour. Microhardness of the exposed surface is slightly decreased with further increase of the exposition dose. It can be caused by

XRD showed that only WC phase is registered on the initial surface of WC-8Co. The high-temperature carbide phase  $W_2C$  with smaller content of carbon is appeared in the surface layer after nitrogen plasma impacts. Simultaneously, the content of WC is considerably decreased. Thus, primary removal of light component-carbon and saturation of surface layer by atoms of tungsten is observed. It can be caused by a selective sputtering of carbon under bombardment of WC-8Co by  $N^+$  ions. In addition, halo is observed in diffraction patterns of irradiated target in the range of  $25^\circ$ - $60^\circ$  of  $2\theta$  angles with maximum located at  $40^\circ$ . This is an indication of amorphous film development on the exposed surface, which may include both carbides and carbonitrides of tungsten and cobalt.

The virgin sample of WC-20Co is characterized by WC and  $\alpha$ -Co phases. The phase structure of WC-20Co after irradiation with nitrogen plasma consists of the main carbide phase WC,  $\alpha$ -Co and appeared small quantity of  $W_2C$ . An oxide phase CoO is not detected. In this case diffractogram has a wide halo area also, which is located in the same range of  $2\theta$  angles.

Modification of thin (0.5-2  $\mu$ m) PVD coatings of MoN, C+W, TiN, TiC, Cr, Cr+CrN and others with the pulsed plasma processing are analyzed also. It is shown that pulsed plasma treatment results in essential improvement of physical and mechanical properties of exposed materials. For example, microhardness of samples with Cr coating, after plasma treatment, increased in 2,5 times [29,30].

Experiments with different steels and cast iron reveal possibility for essential improvement of wear resistance in result of applied combination of coatings deposition with pulsed plasma processing. Alloying of surface layer in result of the coating-substrate mixing in liquid stage allows achievement of desirable chemical composition in surface layers being most loaded in all machine components. In particular, combined plasma processing is found to be prospective for modification of piston rings and other machine parts operating in conditions of bearing or dry friction.

### CONCLUSION

Basic principles of high current plasma accelerators and recent state of their investigations in IPP NSC KIPT are briefly described. In such devices an internal magnetic field is created by high current up to several MA in the discharge and it is used for both plasma flow acceleration up to  $10^3$  km/s.

It is shown that quasi-stationary plasma accelerators (QSPA) are especially attractive systems from the point of view dense plasma generation with super high energy contentment that can be realized in long pulse operational regime, while short pulsed plasma guns have great potential for technological usage due to the high efficiency in combination with their robust design.

Results of simulation experiments relevant to plasma surface interactions in extreme conditions of thermonuclear reactor are discussed emphasizing key physical effects of plasma energy transfer under powerful plasma impacts to the material surface, erosion mechanisms and their contribution under various conditions, dynamics of erosion products as well as and resulting material damage.

Experimental studies of surface modification by pulsed plasma processing using pulsed plasma accelerator (PPA) operating with various working gases have revealed possibility of essential improvements of material properties, increase of microhardness and wear resistance in surface layers in result of plasma treatment, favorable structure changes in modified layers accompanied by material alloying from gas and metallic plasma, as well as due to the mixing process in liquid phase.

### ACKNOWLEDGEMENTS

This paper reviews experimental results obtained in the Laboratory of Plasma Accelerators in IPP NSC KIPT during several years, and, partially, within international collaborations. The contribution of all team members participating in experiments is deeply appreciated.

### REFERENCES

1. Encyclopedia of Low Temperature Plasma. – Vol. III / Ed. V.E. Fortov. – Moscow: Nauka, 2000.
2. Fizika i Primenenie Plazmennyh Uskoritelej. – Minsk: Nauka i Tekhn, 1974. (in Russian).
3. Morozov A.I., Solov'yov L.S. Stationary plasma streams in a magnetic field // Voprosy Teorii Plazmy. – 1974. - Vol.8. - P.3-87. (in Russian).
4. Morozov A.I. Principles of quasistationary plasma accelerators (QSPA) // Sov. J. Plasma Phys. – 1990. - Vol.16 (2). - P. 48.
5. Tereshin V.I. et al. Investigation of powerful quasi-stationary coaxial plasma accelerators with rod electrodes. In book: Ionnye Inzhektoriy i Plazmennye Uskoriteli. – Moscow: Energoatomizdat, 1989. - P.106-123. (in Russian).
6. Voloshko A.Yu. et al. Study of two-stage quasistationary plasma accelerator (QSPA) with rod electrodes // Sov. J. Plasma Phys. – 1990. - Vol.16 (2). - P.85-91.
7. Voloshko A.Yu. et al. Investigation of the local parameters of plasma flow in a two-stage QSPA P-50 //Sov. J. Plasma Phys. - 1990. - Vol.16 (2). - P.91-95.
8. Kulik N.V. et al. Main characteristics of a high-power full scale quasi-stationary plasma accelerator QSPA Kh-50 and some results of preliminary experiments / 18th European Conference on Controlled Fusion and Plasma Phys. - 1991, Contributed papers, part III. - P.41-44.
9. Morozov A.I. et al. QSPA Kh-50 full scale high power quasistationary plasma accelerator // Plasma Devices and Operations. – 1992. - Vol.2. - P.155-165.

10. Tereshin V.I. Quasi-stationary plasma accelerators and their applications // *Plasma Phys. Contr. Fus.* – 1995. - Vol.37. - P.A177-A190.
11. Tereshin V.I. et al. Powerful Quasi-Steady-State Plasma Accelerator for Fusion Experiments // *Brazilian Journal of Physics.* - 2002. - Vol.32, №1. - P.165-171.
12. Volkov Ya.F. et al. Investigation of plasma in cathode transformer of QSPA P-50 // *Sov. J. Plasma Phys.* - 1992. - Vol.18 (11). - P.718-723.
13. Arkhipov N.I. et al. Material erosion and erosion products in disruption simulation experiments at the MK-200 UG facility // *Fus. Eng. and Design.* – 2000. –Vol. 49-50. – P.151.
14. Chebotarev V.V., Garkusha I.E., Garkusha V.V. et al. Characteristics of the transient plasma layers produced by irradiation of graphite targets by high power quasi-stationary plasma streams under the disruption modeling experiments // *J. Nucl. Mater.* - 1996. - Vol.233-237. - P.736-740.
15. Federici G. et al. Assessment of erosion of the ITER divertor targets during type I ELMs // *Plasma Phys. Control. Fusion.* – 2003. – Vol.45. – P. 1523.
16. Loarte A. et al. Characteristics of type I ELM energy and particle losses in existing devices and their extrapolation to ITER // *Plasma Phys. Control. Fusion.* – 2003. – Vol.45. – P.1549.
17. Tereshin V.I., Garkusha I.E., Bandura A.N. et al. Influence of plasma pressure gradient on melt layer macroscopic erosion of metal targets in disruption simulation experiments // *J. Nucl. Mater.* - 2003. - Vol.313-316. - P.686-690.
18. Hirai T., et al. Cracking failure study of ITER-reference tungsten grade under single pulse thermal shock loads at elevated temperatures // *Journ. Nucl. Mater.* – 2009. - Vol. 390–391. - P. 751–754.
19. Garkusha I.E. et al. Latest Results from ELM-simulation Experiments in Plasma Accelerators // *Physica Scripta.* – 2009. - Vol.138. – P.014054.
20. Garkusha I.E. et al. Damage to Preheated Tungsten Targets after Multiple Plasma Impacts Simulating ITER ELMs // *Journ. Nucl. Mater.* – 2009. - Vol.386-388. - P.127-131.
21. Shoshin A.A. et al. Plasma-Surface Interaction During ITER Type 1 ELMs: Comparison of Simulation with QSPA KH-50 and the GOL-3 Facilities // *Fusion Sci. and Techn.* – 2011. - Vol.59, №1. - P.57-60.
22. Ladygina M.S. et al. Spectroscopy of Plasma Surface Interaction in Experiments Simulating ITER Transient Events // *Fusion Sci. and Techn.* – 2011. - Vol.60, №1T. - P.27-33.
23. Garkusha I.E., et al. Properties of modified surface layers of industrial steels samples processed by pulsed plasma streams // *Vacuum.* – 2000. - Vol. 58. - P.195.
24. Tereshin V.I., et al. Pulsed plasma accelerators of different gas ions for surface modification // *Review of Scientific Instruments.* – 2002. - Vol.73. - P. 831.
25. Uglov V.V., et al. Formation of alloying layers in a carbon steel by compression plasma flows // *Vacuum.* – 2007. - Vol. 81. - P.1341.
26. Tereshin V.I., et al. Coating deposition and surface modification under combined plasma processing // *Vacuum.* – 2004. - Vol.73. - P.555.
27. Langner J. et al. Surface modification of constructional steels by irradiation with high intensity pulsed nitrogen plasma beams // *Surface and Coatings Technology.* – 2000. – Vol.128-129. - P.105-111.
28. Makhlay V.A., et al. Features of materials alloying under exposures to pulsed plasma streams // *European Physical Journal D.* – 2009. – Vol.54. - P.185-188.
29. Byrka O.V., et al. Application of pulsed plasma streams for surface modification of constructional materials // *Acta Technica.* – 2011. - Vol.56. – P. T362-T372.
30. Bandura A.N., et al. Alloying and Modification of Structural Materials under Pulsed Plasma Treatment // *International Journal of Plasma Environmental Science & Technology.* – 2011. - Vol.5, №1. - P.2-6.



**Garkusha Igor Evgenijovich**, Dr. Sci, director of Institute of Plasma Physics of the NSC KIPT, professor in V.N. Karazin KhNU, Laureate of State Prize of Ukraine in the field of Science and Technology. Research activities include experimental plasma physics and controlled nuclear fusion, plasma dynamics and diagnostics, plasma-surface interaction and plasma technology (surface modification, coatings deposition, plasma processing in nanotechnology, plasma based EUV lithography), high voltage and vacuum techniques, surface analysis methods. Among the most important results: development and investigations of powerful quasi-steady-state and pulsed plasma accelerators, experimental simulation of ITER plasma loads and fusion materials damage in extreme conditions. He is co-author of “Encyclopedia of Low Temperature Plasma” book, 3 patents and more than 250 scientific publications.